Canadian Journal of Forest Research

OPEN ACCESS | Research Article

Connecting the dots: elucidating the relationship between spruce budworm population dynamics and defoliation

Morgane Henry[a], **Patrick M. A. James**[b], **Daniel D. Kneeshaw**[c], **and Brian Leung**[a,d]

[a]Department of Biology, McGill University, Montréal, QC, Canada; [b]Institute of Forestry and Conservation, John H. Daniels Faculty of Architecture, Landscape and Design, University of Toronto, Toronto, ON, Canada; [c]Center for Forest Research, Université du Québec à Montréal, Montréal, QC, Canada; [d]Bieler School of Environment, McGill University, Montreal, QC, Canada

Corresponding author: **Morgane Henry** (email: morgane.henry2@mail.mcgill.ca)

Abstract

Spruce budworm (*Choristoneura fumiferana*) outbreaks are a major disturbance in northeastern American forests. Monitoring, forecasting, and mitigating outbreak risks require information on how local population densities translate to defoliation. Given landscape-scale heterogeneity, forest structure, and local population dynamics, one expects the relationship between population densities and defoliation to vary spatially and temporally. We analyzed 17 years of larval density data from over 1000 locations in Québec, Canada, to investigate how larval densities and environmental context translate into observable defoliation. We found a positive latitudinal gradient and a positive effect of hardwood species on insect population growth rates. Further, we identified a 3-year cumulative effect of larval densities on defoliation, with a 2-year lag having the strongest influence. On average, a density of 15 larvae per branch corresponded to a 29% probability of defoliation. However, this probability varied widely (13%–52%) with the proportions of balsam fir and black spruce. Our study elucidates the relationship between SBW populations and defoliation, highlighting the importance of cumulative larval density effects and environmental context in defining defoliation risk.

Key words: spruce budworm, insect outbreaks, larval densities, defoliation surveys, population time series

Introduction

Forest insect outbreaks frequently occur synchronously over vast geographical areas and exhibit intricate spatial and temporal dynamics. A multitude of biotic and abiotic factors influence these dynamics, making it difficult to identify clear cause and effect relationships among potential drivers, and to effectively manage outbreaks (Pureswaran et al. 2016). While observable defoliation is often the metric of interest to forest managers, outbreak models relying solely on such data risk missing important aspects of the dynamics, especially during the early phase of an outbreak, when low insect densities begin to increase (Nealis and Régnière 2004; Régnière et al. 2019). Low-density populations, which are below the detection threshold of visible defoliation, are fundamental to the development of the entire outbreak and hold strong potential to further refine efforts to reduce the impact of outbreaks on forest resources. However, low-density, endemic phase populations are difficult to study (Pureswaran et al. 2016; Nenzén et al. 2018). Understanding the relationship between insect population density, the appearance of defoliation, and its effect on forest function is fundamental to making accurate predictions of outbreak development (Johns et al. 2019; Régnière et al. 2023). Further, explicit consideration of how the relationship between population dynamics and visible defoliation varies across environmental conditions is essential to improve outbreak predictions.

Outbreaks of native insects are one of the primary disturbances of North American forests (Kneeshaw et al. 2024). These outbreaks play an essential ecological role and cause large-scale defoliation, thus influencing forest succession and dynamics (Leduc et al. 2021), carbon fluxes (Kurz et al. 2008), but also forest hydrology (Sidhu et al. 2024) and wildfire dynamics (James et al. 2017). The Eastern spruce budworm (SBW, *Choristoneura fumiferana* Clemens) is the most damaging insect defoliator affecting Canadian forests (Natural Resources Canada 2022). Its primary hosts are balsam fir (*Abies balsamea* (L.) Mill.) and spruce species (Picea spp.). Cyclic SBW outbreaks lead to the defoliation of millions of hectares of forest, causing significant growth loss and mortality after years of sustained defoliation, thereby inducing major economic losses (Nealis and Régnière 2004; Chang et al. 2012; MFFP–Ministère des Forêts, de la Faune et des Parcs 2020).

Tree defoliation is a direct outcome of budworm population dynamics and can be used to infer key aspects of those dynamics (Nenzén et al. 2018). However, surveys focused solely on defoliation risk overlooking important demographic dynamics that can strongly influence outbreak development (Pureswaran et al. 2016). One of the main factors influencing observed defoliation is forest composition, par-

ticularly the proportion of host and non-host species (Candau and Fleming 2005; Gray 2013; Bouchard and Auger 2014). Different tree species vary in susceptibility and vulnerability to SBW, which in turn influences defoliation patterns (Hennigar et al. 2008). Furthermore, forest composition affects communities of natural enemies and larval dispersal loss, which also shapes defoliation patterns (Eveleigh et al. 2007; Zhang et al. 2020).

SBW populations are influenced by a variety of drivers, whether biotic or abiotic (Régnière and Nealis 2008; Li et al. 2020). Resource availability (i.e., the quantity of foliage) and the effect of natural enemies have been shown to affect the survival of early instar larvae (Régnière and Nealis 2008). In addition, climate, especially temperature, is known to affect SBW dynamics (Li et al. 2020), influencing both larval survival and mortality (Pureswaran et al. 2016; Marshall and Roe 2021), the timing of larval emergence (i.e., phenology) relative to host trees (Bellemin-Noël et al. 2021), and spatial distribution (Gray 2008; Candau and Fleming 2011; Régnière et al. 2012). Such analyses of drivers of SBW population dynamics have generally been studied locally (often at the stand scale) or over short time scales, and have typically focused on high insect density stages because of the challenges associated with sampling low-density populations (Régnière and Nealis 2008; Pureswaran et al. 2016; Li et al. 2020). Although studies on the effects of environmental conditions on SBW dispersal or outbreak synchrony have been conducted at larger scales and high larval densities using pheromone trap data (Anderson and Sturtevant 2011; Bouchard et al. 2018) and molecular markers (Larroque et al. 2019), further research is needed to evaluate the influence of environmental factors on rising larval densities at the outbreak scale.

Despite their critical role in outbreak development, low but increasing SBW populations and how they link to later spatial patterns of defoliation and tree mortality remain understudied. Disentangling these complex relationships and the influence of environmental context is further complicated by temporally varying lags between increases in population density and observable defoliation (Nealis and Régnière 2004). Although these temporal lags have been noted in the literature (e.g., Régnière et al. 2019; Germain et al. 2021), a comprehensive analysis of this phenomenon is still lacking. Resolving the precise relationship between increasing SBW densities and the appearance of defoliation and tree mortality is a necessary next step to not only improve our fundamental understanding of this outbreaking system but also to develop effective defoliation forecasts and inform management (Johns et al. 2019). In addition, the insights that can be generated through such an investigation can readily be leveraged when combined with ongoing larval monitoring programs (SOPFIM 2019).

In this study, we investigate the relationship between spruce budworm population dynamics and observed defoliation and how this relationship varies spatially. Our specific goals were to (1) estimate local population growth rates across Québec, a province heavily affected by SBW outbreaks; (2) determine the impacts of spatial and environmental covariates on these population trends; and (3) quantify the time lag between increasing population densities and visible defoliation. To meet these goals, we leverage an exceptional spatial and temporal dataset of second-instar SBW larvae (L2) sampled between 2001 and 2018 across the province of Québec at over 1000 locations. These data were collected during a surveillance program by the Québec *Ministère des Ressources Naturelles et des Forêts* and SOPFIM (*Société de Protection des Forêts contre les Insectes et Maladies*) and provide an unprecedented opportunity to study low-density SBW population dynamics and to improve outbreak forecasting capacity in this native, and economically important insect species.

Methods

Data and study area

Our study focused on the commercial forest region of the province of Québec, Canada, south of 52°N, where the MRNF (*Ministère des Ressources Naturelles et des Forêts*; formerly MFFP, *Ministère des Forêts de la Faune et des Parcs*) established monitoring stations to track spruce budworm outbreaks. This large region has three bioclimatic zones: boreal forest in the northern part, dominated by coniferous species (fir and spruce), deciduous forest in the southern part, and mixed forest in between (MFFP 2021).

Second-instar larvae (L2)—the overwintering stage of SBW—were monitored annually in the fall by the MRNF and SOPFIM. The locations sampled included permanent stations sampled annually and locations sampled depending on the outbreak's state in areas eligible for aerial spraying with biological insecticide (SOPFIM 2019). Between 2001 and 2018, L2s were sampled in 1530 sites across Québec (Fig. 1; Supplementary Table S1). At each location, 75 cm branches were collected from three host trees (mostly from balsam fir (*Abies balsamea* (L.) Mill.) and white spruce (*Picea glauca* (Moench) Voss), but also some black spruce (*P. mariana* (Mill.) B.S.P.) and red spruce (*P. rubens* Sarg.) from which the L2s were extracted in the lab (SOPFIM 2019). For the analyses described below, the number of larvae per branch was averaged by site and year.

Maps of defoliation were derived from aerial surveys and were produced annually in Québec by the MRNF starting in 1967 (MFFP 2020). The defoliation level of host species has been classified since 2014 into light (foliage loss in the upper third of the crown of a few trees), moderate (foliage loss in the upper half of the crown of most trees), or severe (foliage loss throughout the crown of most trees), and before that as light (1%–35%), moderate (36%–70%) and severe (71%–100%), although in practice it can be difficult to distinguish among these categories. For simplicity, we merged the three defoliation levels to produce binary classified polygon layers of defoliated and non-defoliated areas (Bouchard and Auger 2014). Between 2009 and 2018, SOPFIM conducted aerial spraying of biological insecticide (*Bacillus thuringiensis kurstaki*; Btk) to protect valuable stands from the ongoing spruce budworm outbreak (SOPFIM 2021). We extracted the spraying status (not sprayed, sprayed once, or sprayed twice) for each year and location sampled for L2 (SOPFIM 2021). Preliminary analyses indicated no significant effect of insecticide use on SBW population growth or presence of defoliation, which was likely due to the small number of sites treated versus non-treated

and because the goal of insecticide spraying in Québec, under the Foliage Protection strategy, is not to stop outbreaks but to keep valuable stands alive until harvest. Therefore, insecticide use was not included in further analyses.

Each sample site was described in terms of several environmental factors derived from the SIFORT geospatial database (*Système d'Information Forestière par Tesselle*; Pelletier et al. 2007). This system overlays a grid of 14 ha tesserae onto forest inventories conducted by Québec's Ministère des Ressources Naturelles et des Forêts and assigns forest attributes to the center of each tessera (Pelletier et al. 2007). These inventories are based on aerial photo interpretation combined with supervised classification using ground-truthing sites (MFFP 2015). We used SIFORT to derive the proportion of SBW host species at each site (Supplementary Table S2). We also derived the proportion of hardwood species, which has been shown to affect defoliation intensity (Bouchard et al. 2005; McNie et al. 2023) due to a presumed influence on natural enemies (Eveleigh et al. 2007). Information about tree species proportion in the forest inventories was categorical: the proportion of host species was expressed in four categories (<15%, 15%–25%, 25%–50%, and >50%), and hardwood species proportion in five categories (<15%, 15%–25%, 25%–50%, 50%–75%, and >75%) (Supplementary Table S2). Drainage type at each location was expressed in seven categories (i.e., excessive, fast, good, moderate, imperfect, bad, and very bad). Age class was also extracted from the SIFORT database and was expressed in eight categories (>20, 21–40, 41–60, 61–80, 81–100, >100 years old). When multiple age classes were present in a single location (stratified stand), we considered the age class of the layer with the largest basal area.

The effect of temperature was captured using the average degree-day above 5 °C at each location. This summary climatic variable was shown to be important for SBW outbreak development and was deemed sufficient given the large scale of the study and collinearity with other climatic predictors (Gray 2008; Bouchard and Auger 2014). Temperature was interpolated at each site, and the number of degree-days above 5 °C was calculated using weather station data and the software BioSIM-11 (Régnière et al. 2017). The interpolations relied on data from 494 weather stations closest to each site, as well as the latitude and elevation of the site (Régnière et al. 2017).

Elevation and slope have been previously identified as important to defoliation trends (Bouchard and Auger 2014; Senf et al. 2017). To assess the influence of topography on population growth, we extracted the elevation at each site from a Digital Elevation Model produced by the Shuttle Radar Topography Mission (SRTM) (mean = 339.4 m, range = 0; 1098 m) (Earth Resources Observation and Science (EROS Center 2017)). We then used QGIS (v. 3.22.7; QGIS Development Team 2020) to derive the slope at each location using the tool *Slope* (mean = 4.92°, range = 0; 56.25°). All remaining analyses were performed in R (v. 4.3.3; R Core Team 2024).

Population trends

Estimating population trends in these L2 time series was challenging because of their irregular sampling. The spatial extent of the samples was not consistent through time, the time series themselves were not all the same length, and some series were missing years. To account for this variability, we used a robust method developed by Humbert et al. (2009), which is an adaptation of the exponential growth state-space model. This model has been shown to perform well and reliably even in the presence of missing data and with different sources of variation (Humbert et al. 2009). The model can be represented as:

$$(1) \quad X(t) = X(t-1) + \mu + E_t$$

$$(2) \quad E_t \sim normal\left(0, \sigma^2\right)$$

Here, $X(t)$ represents the unobserved log-population densities in year t, μ is the trend parameter (overall population growth rate at a location between 2001 and 2018), and E_t represents random perturbations (environmental variability) (Humbert et al. 2009). The observation errors (F_t) are then added to each $X(t)$:

$$(3) \quad Y(t) = X(t) + F_t$$

$$(4) \quad F_t \sim normal\left(0, \tau^2\right)$$

To obtain reliable trend estimates, we only considered time series with at least 10 years of observations. This resulted in estimating growth rates at 591 sites across Québec (Fig. 2).

After estimating the growth rates at each location, we assessed the influence of environmental factors on the population trends using linear models. The environmental factors that we explored for inclusion in our model of population growth were selected based on the literature (Candau and Fleming 2005; Bouchard and Auger 2014; McNie et al. 2023). The predictors included topographic information (elevation and slope), soil moisture regime, climatic data (average degree-day >5 °C, and the proportion of tree species at the site (balsam fir, black spruce, white spruce, and hardwood species) (Dupont et al. 1991; Senf et al. 2017). The predictors were standardized before the analyses. We used a backward selection approach by keeping the significant terms using the threshold $\alpha = 0.05$.

Modelling defoliation and time lag

Defoliation at a site lags behind the initial rise in insect densities, becoming noticeable only after larval populations reach levels sufficient to cause visible damage (Nealis and Régnière 2004; Germain et al. 2021). Understanding the context and timing of defoliation in relation to L2 densities is essential to monitor, forecast, and mitigate outbreak risks, as defoliation and tree mortality result from complex interactions involving site conditions, past defoliation, host availability, weather, climate, predation, and SBW density (Pureswaran et al. 2016; Régnière et al. 2019).

The lag effect of L2 densities on defoliation was tested by correlating defoliation with densities in earlier individual years as well as the cumulative effects of L2s across multiple years. First, we tested the impact of single-year L2 densities on annual defoliation, every year from lag 1–5 years. Then,

we tested the effect of cumulative years on the observed defoliation. We also fit additional parameters for each lag year to test for potential differences in terms of the relative impact of each year using an optimization algorithm (*optim* in R; R Core Team 2024). This functional form was expressed as

$$L_{i,t} = \sum_{x=1}^{5} \lambda_{i,t-x} ln\,(N_{i,t-x} + 1) \quad (5)$$

where λ are the estimated weight parameters for each annual time lag (t) such that all λ summed to one. N represents larvae density at location i, year t, and lag x. We added a $+1$ in the natural logarithm term to avoid undefined values when no larvae were detected at a specific time and location.

We fit mixed-effects logistic regressions using the *lme4* package, where the response variable was the presence or absence of observed defoliation and where "site" was included as a random variable to account for repeated measures (Bates et al. 2015). The new lagged L2 predictor (L from eq. 5) was included in the model, as well as predictors of forest structure (proportion of host species and hardwood species). Finally, we forced a first-order temporal covariate, namely the defoliation status of the previous year, into the models to account for temporal autocorrelation. The optimal model was selected from among the models with different time lag forms and environmental predictors by minimizing the value of AIC using an information-theoretic approach (Burnham and Anderson 2004). The marginal and conditional R^2 of the final selected model were calculated using the R package *MuMIn* (Bartoń 2024).

Effect of ecozone

To assess whether the relationship between lagged SBW densities and defoliation, specifically the time lag functional form, varies regionally, we repeated the analyses described above by stratifying the data by ecozone where both defoliation and L2 data were available (i.e., Atlantic Maritime and Boreal Shield; Fig. 1). Since we were interested in the potential regional differences in the timing between increasing SBW densities and subsequent defoliation, we built separate models instead of including ecozone as a covariate. Differences among regions were then evaluated by comparing the weights λ estimated by the optimization procedure for each ecozone.

Model performance

Using the estimated local population growth rates, we forecast local population densities for 2019 and 2020 at 496 locations where L2 densities were measured between 2016 and 2018. The estimated densities were then compiled into a single predictor (lagged L2 using eq. 5) and added to the mixed-effects logistic regression, including the relevant environmental variables (proportion of balsam fir and black spruce, see Results) to predict the probability of defoliation at each site.

We then compared the predicted defoliation probabilities to the true defoliation status recorded by aerial surveys (MFFP 2020) and assessed the model performance using ROC (receiver operating characteristic) curve, PR (precision–recall) curve, and AUC (area under the curve) using the *precrec* R package (Saito and Rehmsmeier 2017). A ROC curve shows the performance of a binary classification model by plotting the true positive and the false positive rates at different threshold values. The PR curve illustrates the trade-off between precision and recall for different thresholds; high precision is associated with a low false positive rate, while a high recall is related to a low false negative rate.

Results

Population trends

Spruce budworm L2 densities ranged from 0 to a maximum of 774 larvae on a single branch observed in 2018 in a site located in Québec Côte-Nord (Supplementary Table S1). We found that SBW growth rates ranged from −0.57 to 0.86 across Quebec between the years 2001 and 2018, with an average of 0.26 (Fig. 2). Most local populations (86%) showed positive growth rates. The best model to explain local growth rates included four predictors: latitude, elevation, hardwood proportion, and slope ($R^2 = 0.45$, $F_{[5,585]} = 100.5$, $p < 0.001$; Table 1; Fig. S1). While the models showed no two-way interactions, a three-way interaction between elevation, hardwood proportion, and slope was significant ($\beta = 0.015$, SE $= 0.007$, $t(585) = 2.201$, p value $= 0.028$). The latitudinal gradient was the strongest correlate ($R^2_{\text{partial}} = 0.43$; Table 1; Fig. S1), with faster population growth at higher latitudes. Additionally, contrary to previous findings, the proportion of hardwood in the stand was positively correlated with SBW population growth rates; faster population growth (between 2001 and 2018) seems to be linked to a higher proportion of hardwood species (Table 1).

Defoliation model

The proportion of sites exhibiting any level of defoliation varied annually but increased as the outbreak progressed, reaching 31% in 2018, of which 18% showed moderate or severe defoliation (Table S1). We found that the relationship between SBW density and defoliation was dependent on both environmental and temporal factors. Temporally, the occurrence of defoliation showed a time lag wherein SBW densities from 2 years past were most predictive of defoliation in a given year. However, defoliation was best predicted by a 3-year cumulative effect of SBW density, with relative weights for each year shown in eq. 6 and lag 2-year having the highest relative weight.

$$L_{i,t} = 0.29 \ln (N_{i,t-1} + 1) + 0.59 \ln (N_{i,t-2} + 1) + 0.12 \ln (N_{i,t-3} + 1) \quad (6)$$

Only 3 preceding years needed to be considered, as earlier years had virtually no effect (weights ~0) and thus were not influential in explaining the observation of defoliation (Supplementary Table S3). The analysis of single-year lag L2 densities highlighted the explanatory power of lag 2 years, but the cumulative densities predictor outperformed any single-year lag (Supplementary Table S3). The most parsimonious model contained the lagged L2 predictor (L) and the proportion of balsam fir and black spruce (Table 2). The marginal and conditional R^2_{GLMM} were 0.62 and 0.78, respectively.

Fig. 1. Average densities of spruce budworm (*Choristoneura fumiferana*) second instar larvae at locations sampled in (A) 2006, (B) 2012, and (C) 2018. The three ecozones of Québec below the 52nd parallel (Boreal Shield, Mixedwood Plains, and Atlantic Maritime) are also shown. The maps were created in R (v. 4.3.3; R Core Team 2024), using ecozone shapefiles from the Canadian Council on Ecological Areas (CCEA 2014), and the *basemaps* R package (Schwalb-Willmann 2024). Basemap: Voyager by CARTO © CARTO, map data: © OpenStreetMap contributors.

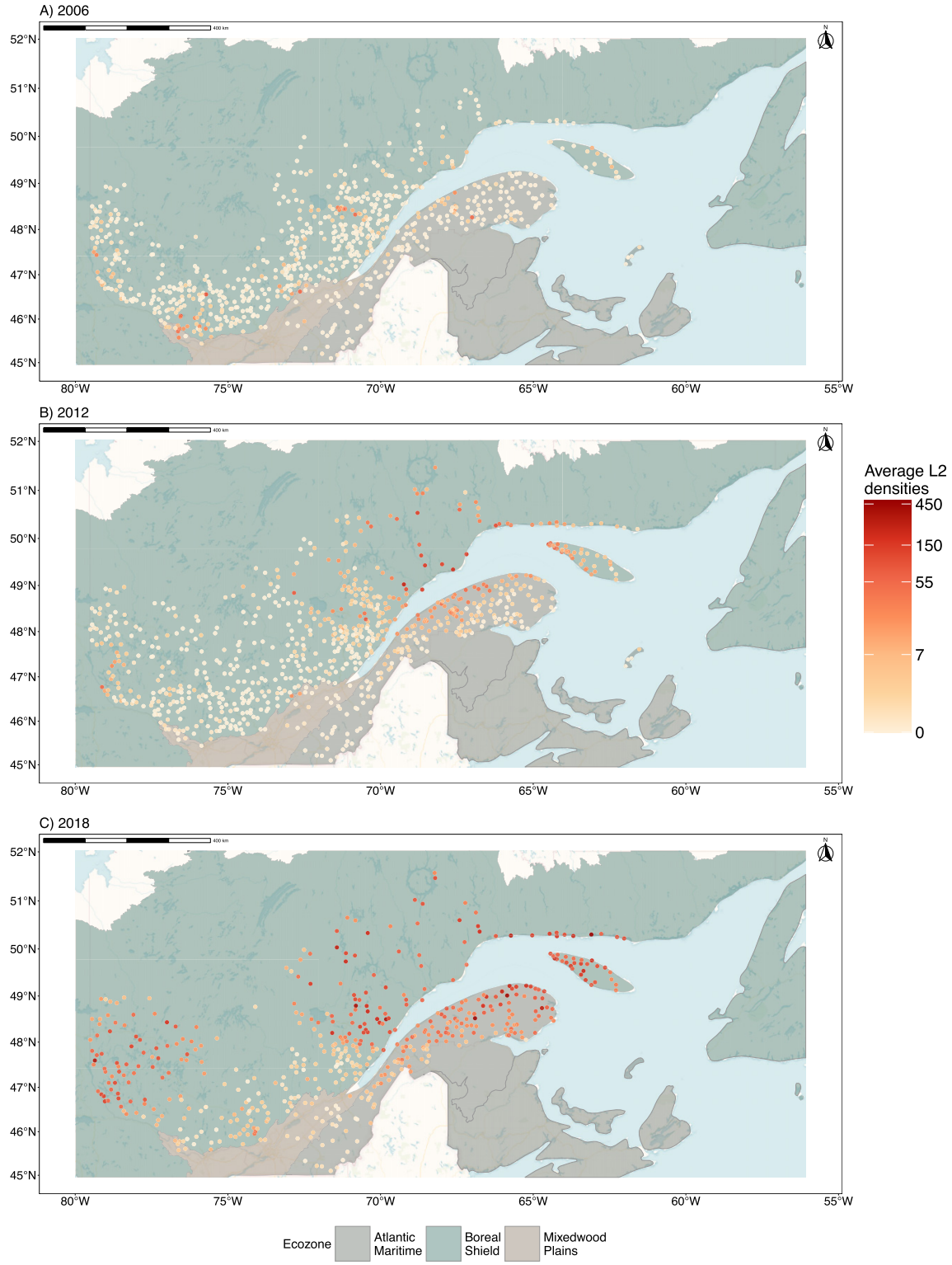

Fig. 2. Map of estimated growth rates of local populations of spruce budworm (*Choristoneura fumiferana*) between 2001 and 2018 during the ongoing outbreak (2006 to present). Positive values correspond to an increase in population density (the higher, the faster), and negative values to a decrease. The map was created in R (v. 4.3.3; R Core Team 2024) using the *basemaps* R package (Schwalb-Willmann 2024). Basemap: Voyager by CARTO © CARTO, map data: © OpenStreetMap contributors.

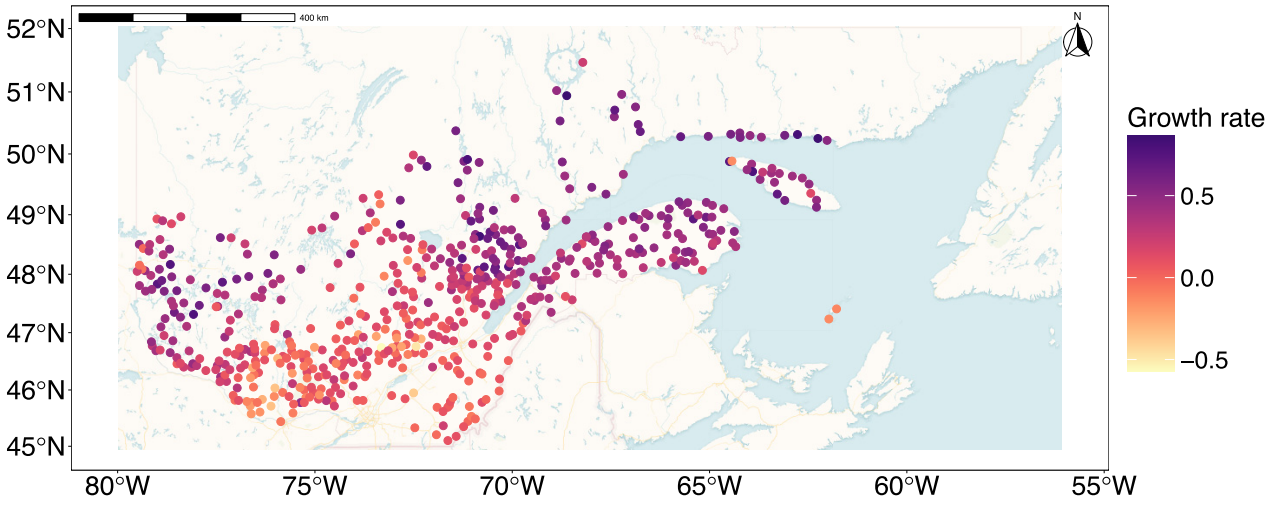

Table 1. We show the partial R^2 of each predictor explaining the growth rates of local spruce budworm (*Choristoneura fumiferana*) populations in Québec between 2001 and 2018.

Predictors	$R^2_{partial}$	Coefficients	SE	Lower CI	Upper CI
Latitude	0.432	0.168	0.008	**0.152**	**0.183**
Hardwood	0.007	0.021	0.008	**0.**005	**0.**035
Elevation	0.003	0.016	0.007	**0.001**	**0.030**
Slope	0.002	− 0.014	0.007	− 0.028	0.0005

Note: The standardized coefficients, standard errors (SE), and 95% confidence intervals (CI) are also presented; CI in bold exclude zero. The predictors were standardized before computing the model.

Table 2. Partial R^2, odd ratios and standard errors (SE) of the predictors explaining the presence or absence of defoliation caused by the current (2006 to present) spruce budworm (*Choristoneura fumiferana*) outbreak in Québec.

Predictors	$R^2_{partial}$	Odd ratios	SE	Lower CI	Upper CI
Lagged_L2	0.29	11.490	1.816	**8.609**	**16.033**
Prev_defol	0.03	9.727	2.225	**6.207**	**15.238**
Balsam fir	0.01	1.364	0.157	**1.089**	**1.718**
Black spruce	0.01	0.573	0.074	**0.440**	**0.732**

Note: "Lagged_L2" represents the cumulative densities of larvae 3 years before recording the defoliation status. "Prev_defol" is a first-order temporal covariate (i.e., the status of defoliation the preceding year) forced into each model. 95% confidence intervals are presented; CI in bold exclude 1. The random effect sites (n = 1093) had a standard deviation of 1.505. The predictors were standardized before computing the model.

Effect of ecozones

We tested whether the relationship between lagged SBW densities and defoliation varied spatially by computing our model optimization separately for two ecozones (Atlantic Maritime and Boreal Shield). The Mixedwood Plains ecozone was not used for this analysis because it contained too few sites to accurately fit the model. Overall, we did not detect significant differences between ecozones. Similar to what we found when using our pooled data, the most influential years were the three preceding defoliation. Generally, the patterns were conserved, with a lag of 2 years having the highest weight in each ecozone (0.63 and 0.54 for Atlantic Maritime and Boreal Shield, respectively; Table 3). Using ecozone-specific lag weights did not improve the model's fit compared to the weights from eq. 6, as informed by AIC ($\Delta AIC_{ecozone\text{-}pooled} = 5.458$). From these results, we concluded that L2 densities have a similar effect on defoliation in both ecozones.

Table 3. Impact of ecozone on the relationship between lagged spruce budworm (*Choristoneura fumiferana*) larvae densities and observed defoliation.

Ecozone	No. of sites	Lag 1	Lag 2	Lag 3
Atlantic Maritime	271	0.27	0.63	0.11
Boreal Shield	792	0.30	0.54	0.17
Mixedwood Plains	21	NA	NA	NA

Note: Lag 1 to Lag 3 represent the lag years, from 1 year before the defoliation status was recorded to 3 years before that. The weights for each lag year were fitted and represented the relative importance of each year to explain defoliation status, with higher weights meaning greater influence in the relationship. The ecozone "Mixedwood Plains" was excluded from this analysis because of a lack of data points.

Predicting defoliation

The defoliation model was built with lagged L2 (from eq. 6) and defoliation data sampled between 2001 and 2018 (Table 2). This model was then used to predict defoliation status at 496 locations in 2019 and 2020 (Fig. 3), and we then compared the predictions to the defoliation maps derived from aerial surveys to assess prediction accuracy. The overall accuracy of the defoliation level classification was 0.91 and 0.78 for 2019 and 2020, respectively. The model showed good predictive performances with ROC and PR AUC values of 0.97 and 0.95, respectively, for the 2019 defoliation predictions and of 0.86 and 0.74 for the 2020 predictions. While the model used defoliation as a binary response, we found a good correspondence between the probability of defoliation and the three defoliation levels (light, moderate, and severe) reported by the MRNF (Fig. 4). The median probability of defoliation was 0.003, 0.82, 0.95, and 0.98 for no defoliation, light, moderate, and severe defoliation, respectively (Fig. 4).

Finally, we showed that forest composition—in particular, the proportions of balsam fir and black spruce—strongly influenced the relationship between increasing L2 densities and future probability of defoliation (Fig. 5), and that defoliation probability varied substantially for a specific L2 density (Fig. 6). As an example, a density of 15 larvae per branch led to an average probability of defoliation of 44%. However, this defoliation risk was as low as 18% in stands with a low proportion (<15%) of balsam fir and a high proportion (>50%) of black spruce and reached 75% in stands with a high proportion of balsam fir and low proportion of black spruce (Fig. 6).

Discussion

The spruce budworm system is of significant interest to researchers and forest managers because of its complex dynamics and the substantial economic losses caused by its outbreaks (Pureswaran et al. 2016). Although this system has been extensively studied, the early stages of outbreak dynamics have received less attention (but see Régnière et al. 2019). Early outbreak dynamics can be particularly important as they influence the ensuing outbreak. By considering larval densities alongside defoliation in our analyses, we clarified the relationship between increasing SBW densities and the appearance of defoliation and shed light on the early stages of outbreak development that led to large-scale defoliation and tree mortality. While essential to effective forecasting and risk mitigation (MacLean et al. 2000, 2019), the transition from low-density populations to visible damage is often challenging to study if both data sources (population densities and defoliation) are not available at a large enough scale. The time series population data used in the present study, spanning from very low larvae to outbreak-level densities at a location, enabled us to effectively model the growth rates of local populations across the outbreak scale and offered an unprecedented opportunity to study the early stages of an outbreak at such large spatial-temporal scales.

Population trends and influence of environment

Latitude was the strongest predictor of population growth, with higher estimated SBW population growth rates in northern parts of the province. A latitudinal trend in SBW populations has been previously noted, with initial outbreak centers occurring further north than previous epidemics (Pureswaran et al. 2015; Boulanger et al. 2025). Furthermore, outbreaks have been observed (MFFP 2020) and predicted (Gray 2008; Régnière et al. 2012) to shift northward, potentially in response to the influence of climate change (Williams and Liebhold 1997; De Grandpré et al. 2018; Boulanger et al. 2025). At least two mechanisms are thought to influence the latitudinal range of the species (Candau and Fleming 2005; Régnière et al. 2012). Warm conditions reduce overwintering survival and influence the southern limit of an outbreak (Régnière et al. 2012). At higher latitudes, the moth's ability to complete its life cycle before it freezes is critical and reflects the northern limit (Régnière et al. 2012). However, our study suggests that other factors related to latitude may be at play beyond temperature. Even though latitude and temperature are highly correlated, the model with latitude still explained 10% more variation than a model where temperature replaced latitude. This might potentially occur because of factors that also correlate with latitude, such as photoperiod, a different or smaller natural enemy complex, or if latitude is a better proxy for more complex effects of growing season length, temperature extremes, or evapotranspiration on population growth (Weber et al. 1999; Régnière et al. 2012; Bouchard and Auger 2014; Marrec et al. 2018; Marshall and Roe 2021). In addition, the current outbreak epicentres were located at northern latitudes (e.g., Québec Côte-Nord), which would influence the rate of growth of neighbouring populations because of proximity to source populations and dispersal from high-density sites (Anderson and Sturtevant 2011; Bouchard and Auger 2014). This could, in turn, exacerbate the latitudinal gradient we observed.

We also found that elevation influences local population growth rates, which is consistent with previous work that examined defoliation patterns (Bouchard and Auger 2014). Elevation is expected to affect insect populations through its influence on temperature and host species (Hodkinson 2005). The weak but positive relationship between eleva-

Fig. 3. Estimated probabilities of defoliation due to the current spruce budworm (*Choristoneura fumiferana*) outbreak (2006 to present) for the years 2019 (A) and 2020 (B). The black squares indicate sites not aerially surveyed for defoliation that year. The maps were created in R (v. 4.3.3; R Core Team 2024) using the *basemaps* R package (Schwalb-Willmann 2024). Basemap: Voyager by CARTO © CARTO, map data: © OpenStreetMap contributors.

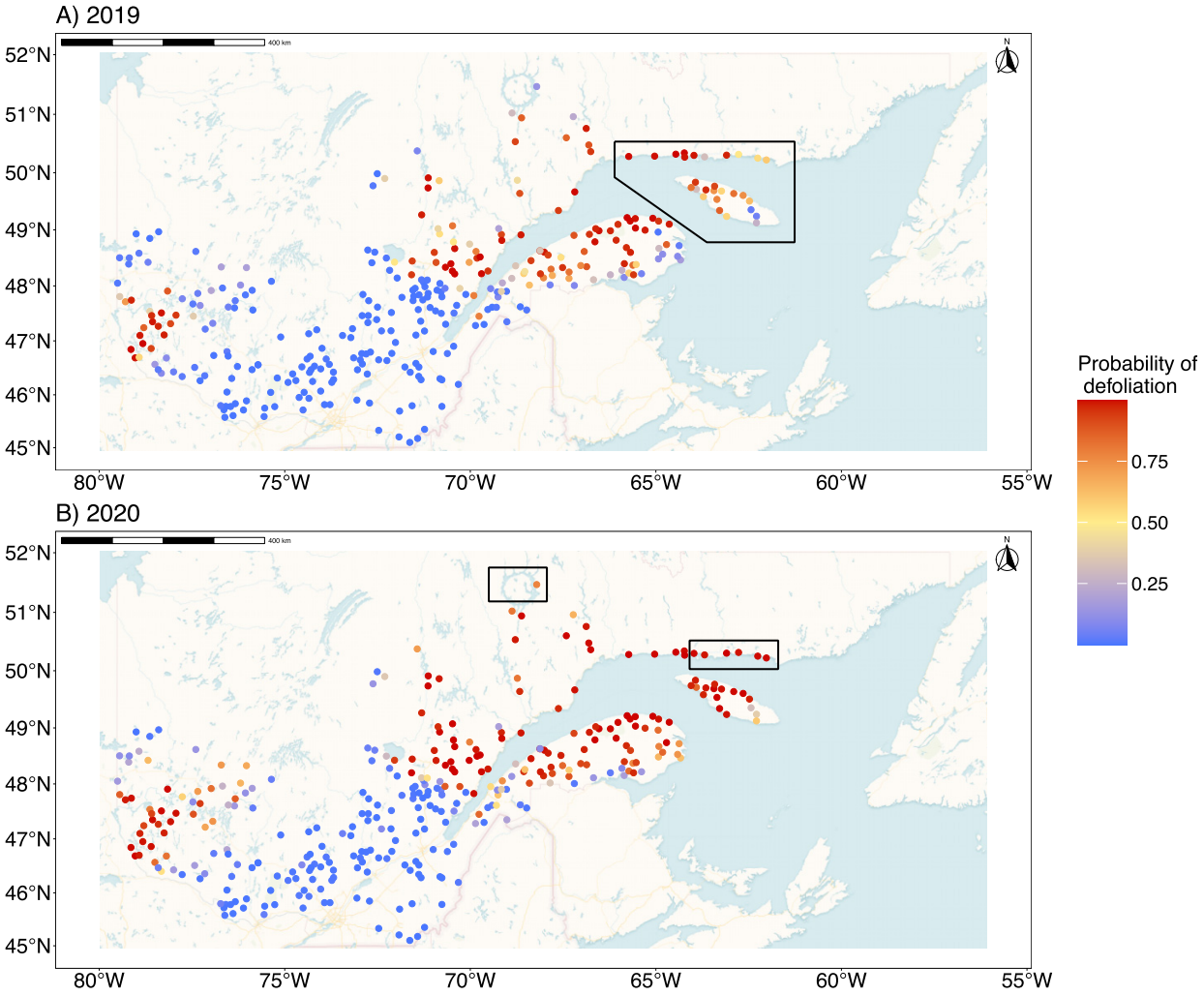

tion and growth rates could be explained in part by more suitable, colder temperatures at higher elevations, in contrast to warmer temperatures at low elevations, which can lead to a decrease in overwintering survival (Régnière et al. 2012).

Finally, we did not find evidence that the proportion of host species influences population growth rates (but it did affect defoliation as addressed below). Although previous work highlighted the importance of host species due to varying phenological matches or mismatches (Nealis and Régnière 2004), we found no such effects, consistent with Li et al. (2020). Our results showed that the proportion of hardwood species was positively correlated with higher growth rates. This was surprising since hardwood species are often identified in the literature as having greater parasitoid richness and parasitism rates, which are expected to have negative impacts on SBW populations (Cappuccino et al. 1998; Eveleigh et al. 2007; Marrec et al. 2018; Zhang et al. 2018). However, a recent study (McNie et al. 2023) found that a higher relative content of hardwoods at the landscape scale was associated with an increased risk of defoliation onset, contrary to the previously described protective effect of hardwood species at the local scale. One potential explanation could relate to a resource dilution effect, where stands with a higher proportion of hardwood species result in a higher concentration of larvae on relatively few host trees, leading to higher densities per branch and potentially explaining the positive effect of hardwood proportion (Bognounou et al. 2017). Another potential explanation is a delayed response by parasitoid natural enemies during the early phase of the increase in SBW populations. This delay may arise as parasitoids gradually aggregate in areas of increasing SBW density and shift away from alternative lepidopteran hosts (Eveleigh et al. 2007). Taken together, these mechanisms may help explain the relatively weak positive relationship observed between hardwood proportion and defoliation.

Fig. 4. Relationship between the predicted probabilities of defoliation in 2019 caused by spruce budworm (*Choristoneura fumiferana*) in Québec with the observed defoliation levels from aerial surveys of defoliation conducted by the Ministry of Natural Resources and Forests (MRNF).

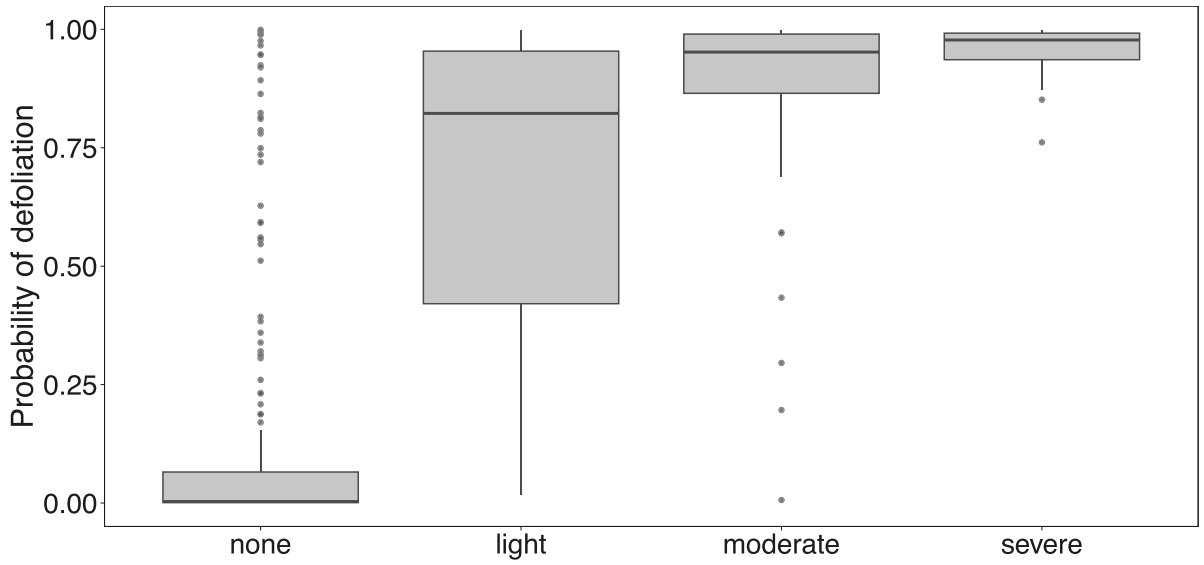

Fig. 5. Relationship between the probability of defoliation in 3 years and the L2 densities observed per branch. The solid line represents forest stands with high (≥50%) proportions of balsam fir (*Abies balsamea*) and low proportions (<15%) of black spruce (*Picea mariana*). The dashed line represents forest stands with low proportions (<15%) of balsam fir and high proportions (≥50%) of black spruce.

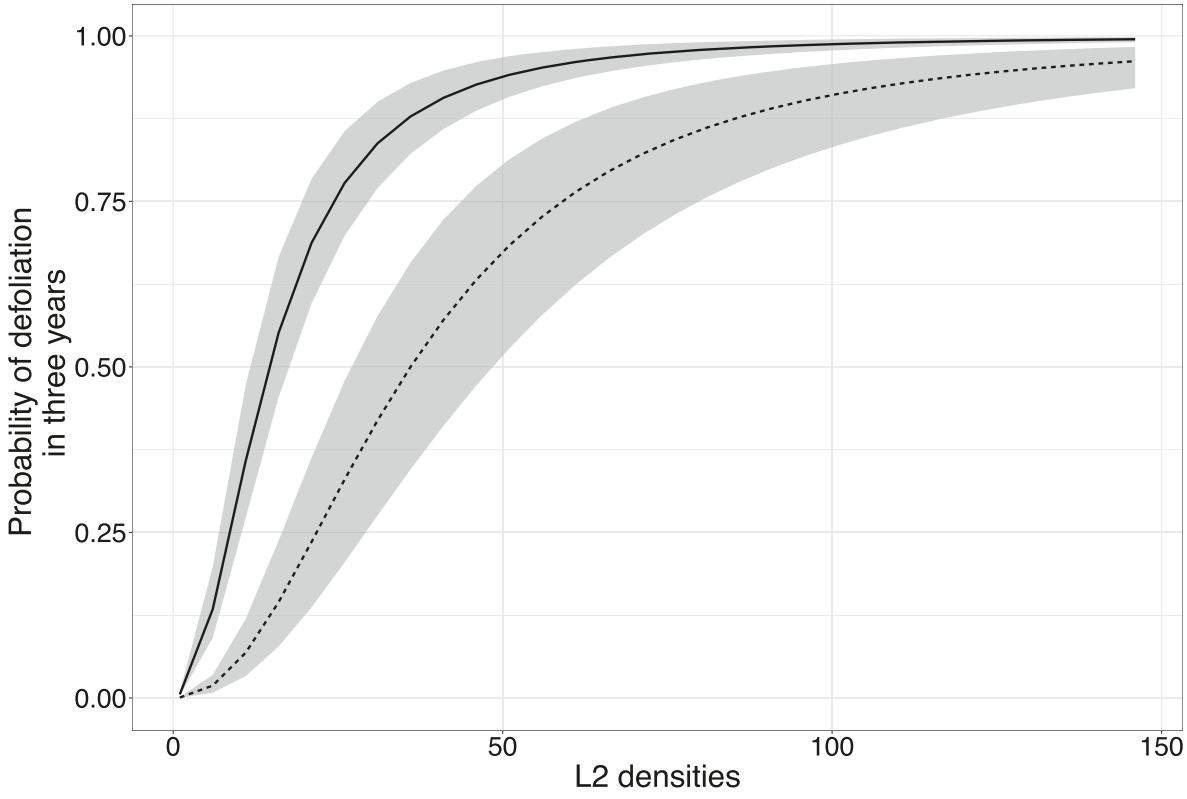

Larvae densities and defoliation

The impact of outbreaking insects on their hosts may not be immediately apparent, as the damage only becomes visible once a high enough density of feeding larvae is reached (Régnière et al. 2019). We explicitly searched for and detected a time lag of effect such that larval SBW density 2 years

Fig. 6. Predicted probabilities of defoliation in 3 years depending on different spruce budworm (*Choristoneura fumiferana*) larvae densities per branch and forest composition at the location of interest. The forest composition is expressed as the proportion of balsam fir (*Abies balsamea*) and black spruce (*Picea mariana*) in three different classes (low, intermediate, and high). The defoliation status at the previous time step (temporal covariate included in the model) was set to "no defoliation" to capture the probability of transitioning from not defoliated to defoliated.

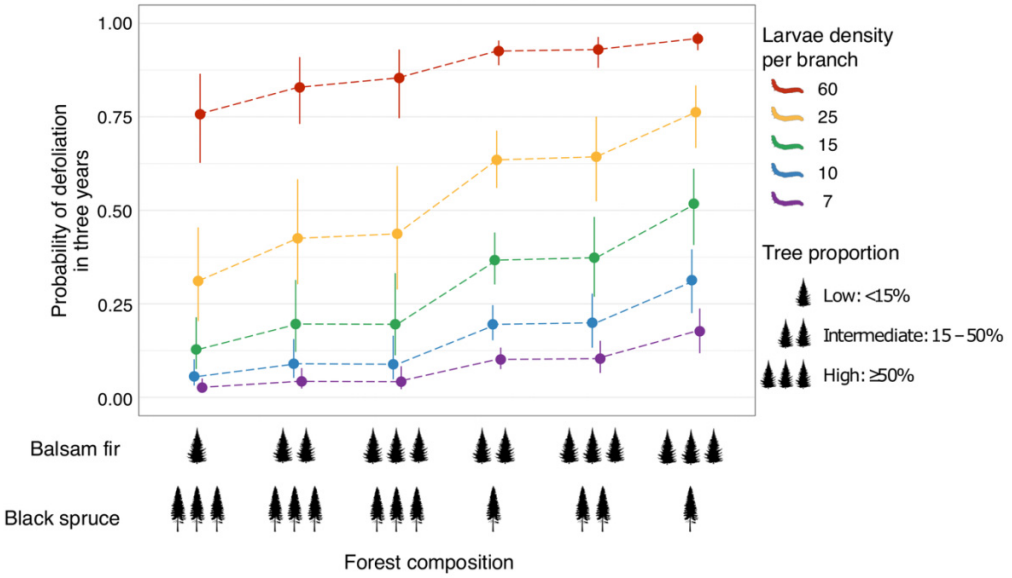

before the observation of defoliation had the largest influence on the probability of defoliation. While larval density 2 years before defoliation was a strong predictor of single-year impacts, the cumulative densities of larvae over the 3 years preceding defoliation best explained defoliation patterns. This result remained consistent across ecozones, indicating that the relationship between increasing local population densities and the onset of defoliation holds throughout the outbreak range in Québec. This lag indicates a temporal delay between the transition of SBW larvae to outbreaking densities and the detectability of an outbreak by aerial surveys (Germain et al. 2021). Identifying this lag enhances our understanding of the critical transition phase and provides valuable insights into the early-stage dynamics of an outbreak.

To date, studies investigating a temporal lag have relied on data from 1 year to predict outbreak conditions in the following year (Li et al. 2020; Régnière et al. 2023). Outbreaks are inherently temporal processes, with current conditions shaped by previous years (Kneeshaw et al. 2024). Characterizing interannual dynamics and how increasing population densities lead to defoliation is critical for understanding outbreak development and improving predictive models. In our study, the 3-year cumulative lag increases the window of opportunity to predict defoliation risk before damage occurs. This aligns with the time frame described in Germain et al. (2021), where they showed that the presence probability of certain bird species (mostly bay-breasted warblers (*Setophaga castanea*)) increased 3–4 years before observing defoliation. Using the time lag described here, together with data from the L2 monitoring program, represents a significant improvement in our capacity to forecast outbreak risk and identify areas at high risk of future defoliation.

Defoliation and forest composition

Besides the lagged densities of L2, forest composition was found to be an important predictor of defoliation, in particular the proportions of balsam fir and black spruce. The positive relationship between defoliation and the proportion of balsam fir was expected and is well-known in the SBW literature (Bouchard et al. 2005; Hennigar et al. 2008; Bouchard and Auger 2014). Balsam fir is the preferred host of SBW, and the matching phenology between larval emergence and budburst makes it the most susceptible and vulnerable species to SBW defoliation (Hennigar et al. 2008).

Defoliation decreased as the proportion of black spruce increased, as previously described (Blais 1957; Hennigar et al. 2008). Budburst in black spruce is typically later than that of balsam fir, which results in less synchronized phenologies between budworm and host and limits the overall defoliation (Hennigar et al. 2008). That phenological mismatch also leads to a lower rate of development and an increased mortality rate of larvae when they feed on black spruce (Blais 1957). McNie et al. (2023) found that a higher relative proportion of black spruce decreases the risk of outbreak onset and ensuing mortality. However, Bellemin-Noël et al. (2021) showed that climate change could disrupt that relationship by inducing earlier black spruce budburst following higher temperatures, leading to a better synchronization with budworm emergence and an increased vulnerability to SBW defoliation.

We observed a negative relationship between defoliation and the proportion of black spruce, which does not indicate better synchronization. However, we did observe a strong latitudinal gradient in SBW growth rates, which could be a glimpse into a future where SBW are performing well at higher latitudes. Outbreaks are predicted to shift their limit northward in black spruce dominated boreal forests (Candau and Fleming 2011; Régnière et al. 2012), which could cause larger outbreaks if the phenological match between black spruce and spruce budworm improves (Pureswaran et al. 2015; Bellemin-Noël et al. 2021). An increase in outbreak severity and host-tree mortality in northern black spruce forests could modify ecosystem dynamics, leading to a range of consequences, from forest productivity and resilience, disturbance interactions, and economic impacts (Pureswaran et al. 2015). Further research is needed to improve our understanding and forecasts of how spruce budworm populations, their host trees, and natural enemies will respond to the changing climate in the coming decades, and consequently, whether the severity of future outbreaks is likely to increase or decrease (Pureswaran et al. 2015; Boulanger et al. 2025).

Predicting defoliation

A central aspect of spruce budworm research involves predicting outbreak development, and anticipating defoliation is an important component of this effort. Here, we focused on forecasting defoliation for the current outbreak. We predicted the presence of defoliation in 2019 and 2020 with high accuracy and found that the models performed well. The models integrated L2 densities and forest composition to generate context-specific predictions based on environmental conditions. Notably, the L2 time series provided critical information for proactively assessing defoliation risk. Our findings demonstrate that cumulative larval densities over 3 years offer greater explanatory power. This approach improved prediction accuracy and enabled earlier forecasting of defoliation.

In addition, extensive monitoring of spruce budworm larvae allows for defoliation predictions in areas where aerial surveys were not conducted in a given year. While defoliation maps are primarily generated using aerial surveys and, more recently, satellite imagery (MFFP 2020), L2 densities can help address gaps in these maps. For example, Anticosti Island was not surveyed for defoliation in 2019, but we forecast the probability of defoliation in 2019 with the L2 densities monitored in previous years and given the location-specific forest composition (Fig. 3). While forest managers may have anticipated some amount of defoliation in the year not surveyed given the proximity to defoliated sites in the previous year, our model provides more fine-tuned predictions based on larvae densities and environmental factors and suggests that defoliation should have been surveyed.

Furthermore, the predicted probabilities of defoliation corresponded to the three defoliation levels used in Québec (MFFP 2020). Light defoliation showed a broad range of probabilities, which was not surprising given the lower reliability of accurately classifying forests with less than 30% defoliation (MacLean and MacKinnon 1996). Importantly, the relationship was especially strong for moderate and severe defoliation, which are often the levels of interest. Specifically, the average L2 density associated with the median probability of moderate defoliation in the most vulnerable stands (high and low proportions of balsam fir and black spruce, respectively) was 50 L2. Alternatively, a more conservative estimate corresponding to the first quartile of moderate defoliation was a density of 34 L2 per branch. In the contrasting forest composition scenario (low and high proportions of balsam fir and black spruce, respectively), the L2 densities corresponding to moderate defoliation were much higher, as expected (Blais 1957; Hennigar et al. 2008). Notably, we see a sharp increase in defoliation probability as soon as the L2 densities start to increase for the most vulnerable stands.

While we present L2 values associated with at least moderate defoliation, they should be treated with caution. These values are not conservative estimates, and once the L2s reach these densities, some level of defoliation will likely have occurred. Additionally, our analysis focuses on a 3-year time window where the conditions are assumed constant, but populations grow, and the probability and severity of defoliation can change over time. A more complete approach, and avenue for future research, could develop a broader, temporally explicit risk framework that integrates environmental factors, prior defoliation, and population dynamics.

As a potential future direction, researchers could explore the application of our findings to management. For instance, our model suggests that early forecasts of defoliation risk are possible, upto 3 years before defoliation becomes visible, providing a longer timeframe for planning responses. This could potentially offer benefits for management strategies focusing on protecting valuable stands until harvest (i.e., foliage protection) (MacLean et al. 2001), although given the maturity of current SBW management programs, any potential change would need to be considered carefully with further analyses.

Conclusion

The present study is one of the first efforts to explore the relationships between low but rising insect densities and defoliation across a SBW outbreak range. Understanding this relationship is essential to better predict outbreak development and accurately forecast the occurrence of defoliation. We leveraged long-term surveillance data of early instar larvae densities collected across Québec to develop novel insights into the dynamics of a forest insect outbreak from onset to nearing its peak. The latitudinal gradient identified in the population growth rates shows enhanced SBW performance in the northern parts of the epidemic, which could illustrate the impacts of climate change on the SBW system. The best predictor of defoliation emerged when considering the cumulative influence of larval densities over 3 years. Although defoliation is typically the metric of interest, we show the value of monitoring early instar larvae and recommend including cumulative insect densities in outbreak models to enable earlier defoliation forecasts.

Acknowledgements

We thank the Québec *Ministère des Ressources Naturelles et des Forêts* (QMRNF) and Pierre Therrien for providing the data on spruce budworm larvae densities. This study was funded by an FRQNT Team Grant to D. Kneeshaw, P. M. A. James, and B. Leung.

Article information

History dates

Received: 29 June 2025
Accepted: 19 February 2026
Accepted manuscript online: 3 March 2026
Version of record online: 15 April 2026

Data availability

The code is available from the corresponding author upon request. The L2 data analyzed during this study were generously provided by the Québec Ministère des Ressources Naturelles et des Forêts (QMRNF). Data are available from the authors upon reasonable request and with permission of the QMNRF.

Author information

Author ORCIDs

Morgane Henry https://orcid.org/0000-0003-0946-6256

Author contributions

Conceptualization: MH, PMAJ, DK, BL
Formal analysis: MH
Methodology: MH, PMAJ, BL
Writing – original draft: MH, PMAJ, BL
Writing – review & editing: MH, PMAJ, DK, BL

Competing interests

The authors declare there are no competing interests.

Funding information

This research was supported by the Fonds de Recherche du Québec Nature et Technologies (Team Grant No. 286905) to D. Kneeshaw, P. M. A. James, and B. Leung.

Supplementary material

Supplementary data are available with the article at https://doi.org/10.1139/cjfr-2025-0197.

References

Anderson, D.P., and Sturtevant, B.R. 2011. Pattern analysis of eastern spruce budworm *Choristoneura fumiferana* dispersal. Ecography, **34**: 488–497. doi:10.1111/j.1600-0587.2010.06326.x.

Bartoń, K., 2024. MuMIn: multi-model inference. R package version 1.48.4. Available from https://CRAN.R-project.org/package=MuMIn [accessed August 2024].

Bates, D., Mächler, M., Bolker, B., and Walker, S., 2015. Fitting linear mixed-effects models using lme4. J. Stat. Soft. **67**. doi:10.18637/jss.v067.i01.

Bellemin-Noël, B., Bourassa, S., Despland, E., Grandpré, L.D., and Pureswaran, D.S. 2021. Improved performance of the eastern spruce budworm on black spruce as warming temperatures disrupt phenological defences. Glob. Change Biol. **27**: 3358–3366. doi:10.1111/GCB.15643.

Blais, J.R. 1957. Some relationships of the spruce budworm, *Choristoneura fumiferana* (clem.) to black spruce, *Picea mariana* (moench) voss. For. Chron. **33**: 364–372. doi:10.5558/tfc33364-4.

Bognounou, F., De Grandpré, L., Pureswaran, D.S., and Kneeshaw, D. 2017. Temporal variation in plant neighborhood effects on the defoliation of primary and secondary hosts by an insect pest. Ecosphere, **8**: e01759. doi:10.1002/ecs2.1759.

Bouchard, M., and Auger, I. 2014. Influence of environmental factors and spatio-temporal covariates during the initial development of a spruce budworm outbreak. Landsc. Ecol. **29**: 111–126. doi:10.1007/s10980-013-9966-x.

Bouchard, M., Kneeshaw, D., and Bergeron, Y. 2005. Mortality and stand renewal patterns following the last spruce budworm outbreak in mixed forests of western Quebec. For. Ecol. Manage. **204**: 297–313. doi:10.1016/j.foreco.2004.09.017.

Bouchard, M., Régnière, J., and Therrien, P. 2018. Bottom-up factors contribute to large-scale synchrony in spruce budworm populations. Can. J. For. Res. **48**: 277–284. doi:10.1139/cjfr-2017-0051.

Boulanger, Y., Desaint, A., Martel, V., Marchand, M., Tonye, S.M., Saint-Amant, R., and Régnière, J., 2025. Recent climate change strongly impacted the population dynamic of a North American insect pest species. PLOS Clim. **4**: e0000488. doi:10.1371/journal.pclm.000048.

Burnham, K.P. and D.R. (*Editors*). 2004. Model selection and multimodel inference. Springer New York, New York, NY. doi:10.1007/b97636.

Canadian Council on Ecological Areas (CCEA). 2014. Ecozones of Canada [Data set]. Available from https://ccea-ccae.org/ecozones-downloads/ [accessed July 2022].

Candau, J.N., and Fleming, R.A. 2011. Forecasting the response of spruce budworm defoliation to climate change in Ontario. Can. J. For. Res. **41**: 1948–1960. doi:10.1139/x11-134.

Candau, J.-N., and Fleming, R.A. 2005. Landscape-scale spatial distribution of spruce budworm defoliation in relation to bioclimatic conditions. Can. J. For. Res. doi:10.1139/X05-078.

Cappuccino, N., Lavertu, D., Bergeron, Y., and Régnière, J. 1998. Spruce budworm impact, abundance and parasitism rate in a patchy landscape. Oecologia, **114**: 236–242. doi:10.1007/s004420050441. PMID: 28307937.

Chang, W.-Y., Lantz, V.A., Hennigar, C.R., and MacLean, D.A. 2012. Economic impacts of forest pests: a case study of spruce budworm outbreaks and control in New Brunswick, Canada. Can. J. For. Res. **42**: 490–505. doi:10.1139/x11-190.

De Grandpré, L., Pureswaran, D., Bouchard, M., and Kneeshaw, D. 2018. Climate-induced range shifts in boreal forest pests: ecological, economic, and social consequences. Can. J. For. Res. **48**: v–vi. doi:10.1139/cjfr-2018-0058.

Dupont, A., Belanger, L., and Bousquet, J. 1991. Relationship between balsam fir vulnerability to spruce budworm and ecological site conditions of fir stands in central Quebec. Can. J. For. Res. **21**: 1752–1759. doi:10.1139/x91-242.

Earth Resources Observation And Science (EROS) Center. 2017. Shuttle Radar Topography Mission (SRTM) 1 Arc-Second Global. doi:10.5066/F7PR7TFT.

Eveleigh, E.S., McCann, K.S., McCarthy, P.C., Pollock, S.J., Lucarotti, C.J., Morin, B., et al. 2007. Fluctuations in density of an outbreak species drive diversity cascades in food webs. Proc. Natl. Acad. Sci. U.S.A. **104**: 16976–16981. doi:10.1073/PNAS.0704301104. PMID: 17940003.

Germain, M., Kneeshaw, D., De Grandpré, L., Desrochers, M., James, P.M.A., Vepakomma, U., et al. 2021. Insectivorous songbirds as early indicators of future defoliation by spruce budworm. Landsc. Ecol. **36**: 3013–3027. doi:10.1007/s10980-021-01300-z.

Gray, D.R. 2013. The influence of forest composition and climate on outbreak characteristics of the spruce budworm in eastern Canada. Can. J. For. Res. **43**: 1181–1195. doi:10.1139/cjfr-2013-0240.

Gray, D.R. 2008. The relationship between climate and outbreak characteristics of the spruce budworm in eastern Canada. Clim. Change, **87**: 361–383. doi:10.1007/s10584-007-9317-5.

Hennigar, C.R., MacLean, D.A., Quiring, D.T., and Kershaw, J.A., Jr. 2008. Differences in spruce budworm defoliation among balsam fir and white, red, and black spruce. For. Sci. **54**: 158–166. doi:10.1093/forestscience/54.2.158.

Hodkinson, I.D. 2005. Terrestrial insects along elevation gradients: species and community responses to altitude. Biol. Rev. **80**: 489–513. doi:10.1017/S1464793105006767. PMID: 16094810.

Humbert, J.-Y., Mills, L.S., Horne, J.S., and Dennis, B. 2009. A better way to estimate population trends. Oikos, **118**: 1940–1946. doi:10.1111/J.1600-0706.2009.17839.X.

James, P.M.A., Robert, L.E., Wotton, B.M., Martell, D.L., and Fleming, R.A. 2017. Lagged cumulative spruce budworm defoliation affects the risk of fire ignition in Ontario, Canada. Ecol. Appl. **27**: 532–544. doi:10.1002/eap.1463. PMID: 27809401.

Johns, R.C., Bowden, J.J., Carleton, D.R., Cooke, B.J., Edwards, S., Emilson, E.J.S., et al. 2019. A conceptual framework for the spruce budworm early intervention strategy: can outbreaks be stopped? Forests, **10**. doi:10.3390/f10100910.

Kneeshaw, D., Sturtevant, B.R., Cooke, B., Work, T., Pureswaran, D., De-Grandpré, L., and MacLean, D.A. 2024. Insect disturbances in forest ecosystems, *In* Routledge Handbook of Forest Ecology. Routledge. doi:10.4324/9781003324072.

Kurz, W.A., Dymond, C.C., Stinson, G., Rampley, G.J., Neilson, E.T., Carroll, A.L., et al. 2008. Mountain pine beetle and forest carbon feedback to climate change. Nature, **452**: 987–990. doi:10.1038/nature06777. PMID: 18432244.

Larroque, J., Legault, S., Johns, R., Lumley, L., Cusson, M., Renaut, S., et al. 2019. Temporal variation in spatial genetic structure during population outbreaks: distinguishing among different potential drivers of spatial synchrony. Evol. Appl. **12**: 1931–1945. doi:10.1111/eva.12852. PMID: 31700536.

Leduc, A., Leduc, A., Kneeshaw, D., Maleki, K., and Bergeron, Y. 2021. Advancing and reversing succession as a function of time since fire and insect outbreaks: an 18 year in situ remeasurement of changes in forest composition. J. Veg. Sci. **32**: e12974. doi:10.1111/jvs.12974.

Li, M., MacLean, D.A., Hennigar, C.R., and Ogilvie, J. 2020. Previous year outbreak conditions and spring climate predict spruce budworm population changes in the following year. For. Ecol. Manage. **458**: 117737. doi:10.1016/j.foreco.2019.117737.

MacLean, D.A., Amirault, P., Amos-Binks, L., Carleton, D., Hennigar, C., Johns, R., and Régnière, J. 2019. Positive results of an early intervention strategy to suppress a spruce budworm outbreak after five years of trials. Forests, **10**. doi:10.3390/f10050448.

MacLean, D.A., Erdle, T.A., MacKinnon, W.E., Porter, K.B., Beaton, K.P., Cormier, G., et al. 2001. The Spruce Budworm Decision Support System: forest protection planning to sustain long-term wood supply. Can. J. For. Res. **31**: 1742–1757. doi:10.1139/X01-102.

MacLean, D.A., and MacKinnon, W.E., 1996. Accuracy of aerial sketch-mapping estimates of spruce budworm defoliation in New Brunswick. Can. J. For. Res. **26**: 2099–2108. doi:10.1139/x26-238.

MacLean, D.A., Porter, K.B., MacKinnon, W.E., and Beaton, K.P. 2000. Spruce budworm decision support system: lessons learned in development and implementation. Comput. Electron. Agric. **27**: 293–314. doi:10.1016/S0168-1699(00)00089-2.

Marrec, R., Pontbriand-Paré, O., Legault, S., and James, P.M.A. 2018. Spatiotemporal variation in drivers of parasitoid metacommunity structure in continuous forest landscapes. Ecosphere, **9**: e02075. doi:10.1002/ecs2.2075.

Marshall, K.E., and Roe, A.D. 2021. Surviving in a frozen forest: the physiology of eastern spruce budworm overwintering. Physiology, **36**: 174–182. doi:10.1152/physiol.00037.2020. PMID: 33904790.

McNie, P., Kneeshaw, D., and Filotas, É. 2023. Landscape-scale patterns of eastern spruce budworm outbreak risk: defoliation onset vs. tree mortality. Ecosphere, **14**: e4684. doi:10.1002/ecs2.4684.

MFFP–Ministère des Forêts de la Faune et des Parcs. 2021. Classification Ecologique du Territoire Québecois. Ministère des Forêts, de la Faune et des Parcs, Secteur des forêts, Direction des inventaires forestiers.

MFFP–Ministère des Forêts, de la Faune et des Parcs. 2020. Aires infestées par la tordeuse des bourgeons de l'épinette au Québec en 2020 (Annual Report). Gouvernement du Québec, Direction de la protection des forêts, Québec.

MFFP–Ministère des Forêts de la Faune et des Parcs. 2015. Norme de stratification écoforestière–Quatrième inventaire écoforestier. Ministère des Forêts, de la Faune et des Parcs, Secteur des forêts, Direction des inventaires forestiers.

Natural Resources Canada. 2022. The state of Canada's forests (Annual Report). Canadian Forest Service, Ottawa.

Nealis, V.G., and Régnière, J. 2004. Insect-host relationships influencing disturbance by the spruce budworm in a boreal mixedwood forest. Can. J. For. Res. **34**: 1870–1882. doi:10.1139/x04-061.

Nenzén, H.K., Peres-Neto, P., and Gravel, D. 2018. More than Moran: coupling statistical and simulation models to understand how defoliation spread and weather variation drive insect outbreak dynamics. Can. J. For. Res. **48**: 255–264. doi:10.1139/cjfr-2016-0396.

Pelletier, G., Dumont, Y., and Bédard, M. 2007. SIFORT: Système d'Information FORestière par Tesselle, Manuel de l'usager. Gouv. Qué. Ministère Ressour. Nat. Faune.

Pureswaran, D.S., De Grandpré, L., Paré, D., Taylor, A., Barrette, M., Morin, H., et al. 2015. Climate-induced changes in host tree–insect phenology may drive ecological state-shift in boreal forests. Ecology, **96**: 1480–1491. doi:10.1890/13-2366.1.

Pureswaran, D.S., Johns, R., Heard, S.B., and Quiring, D. 2016. Paradigms in eastern spruce budworm (Lepidoptera: Tortricidae) population ecology: a century of debate. Environ. Entomol. **45**: 1333–1342. doi:10.1093/ee/nvw103. PMID: 28028079.

QGIS Development Team. 2020. QGIS Geographic Information System. QGIS Association.

R Core Team. 2024. R: a language and environment for statistical computing. R Foundation for Statistical Computing, Vienna, Austria.

Régnière, J., Cooke, B.J., Béchard, A., Dupont, A., and Therrien, P. 2019. Dynamics and management of rising outbreak spruce budworm populations. Forests, **10**. doi:10.3390/f10090748.

Régnière, J., Johns, R.C., Edwards, S., Owens, E., and Dupont, A. 2023. Overwintering spruce budworm population density as predictor of following-year larval density and defoliation on balsam fir. For. Ecol. Manage. **546**: 121380. doi:10.1016/j.foreco.2023.121380.

Régnière, J., and Nealis, V.G. 2008. The fine-scale population dynamics of spruce budworm: survival of early instars related to forest condition. Ecol. Entomol. **33**: 362–373. doi:10.1111/J.1365-2311.2007.00977.X.

Régnière, J., Saint-Amant, R., Béchard, A., and Moutaoufik, A. 2017. BioSIM 11: User's manual. Laurentian Forestry Centre Québec, QC, Canada.

Régnière, J., St-Amant, R., and Duval, P. 2012. Predicting insect distributions under climate change from physiological responses: spruce budworm as an example. Biol. Invasions, **14**: 1571–1586. doi:10.1007/s10530-010-9918-1.

Saito, T., and Rehmsmeier, M. 2017. Precrec: fast and accurate precision–recall and ROC curve calculations in R. Bioinformatics, **33**: 145–147. doi:10.1093/bioinformatics/btw570. PMID: 27591081.

Schwalb-Willmann, J. 2024. basemaps: Accessing Spatial Basemaps in R. R package version 0.0.8. Available from https://CRAN.R-project.org/package=basemaps [accessed January 2025].

Senf, C., Campbell, E.M., Pflugmacher, D., Wulder, M.A., and Hostert, P. 2017. A multi-scale analysis of western spruce budworm outbreak dynamics. Landsc. Ecol. **32**: 501–514. doi:10.1007/s10980-016-0460-0.

Sidhu, H., Kidd, K., Emilson, E., Stastny, M., Venier, L., Kielstra, B., and McCarter, C. 2024. Increasing spruce budworm defoliation increases catchment discharge in conifer forests. Sci. Total Environ. **912**: 168561. doi:10.1016/j.scitotenv.2023.168561. PMID: 37981128.

SOPFIM–Société de protection des forêts contre les insectes et maladies. 2019. Inventaire des larves en hibernation (L2) pour la détermination des niveaux d'infestation et de défoliation anticipés par la tordeuse des bourgeons de l'épinette.

SOPFIM–Société de protection des forêts contre les insectes et maladies. 2021. Documentation Informations géographiques–Blocs traités. Available from https://sopfim.qc.ca/en/information-fight-against-pest-insects/documents/ [accessed 5 June 2021].

Weber, J.D., Volney, W.J.A., and Spence, J.R. 1999. Intrinsic development rate of spruce budworm (Lepidoptera: Tortricidae) across a gradient of latitude. Environ. Entomol. **28**: 224–232. doi:10.1093/ee/28.2.224.

Williams, D.W., and Liebhold, A.M. 1997. Latitudinal shifts in spruce budworm (Lepidoptera: Tortricidae) outbreaks and spruce-fir forest distributions with climate change. **32**: 205–215.

Zhang, B., MacLean, D.A., Johns, R.C., and Eveleigh, E.S. 2018. Effects of hardwood content on balsam fir defoliation during the building phase of a spruce budworm outbreak. Forests, **9**: 530. doi:10.3390/f9090530.

Zhang, B., MacLean, D.A., Johns, R.C., Eveleigh, E.S., and Edwards, S. 2020. Hardwood-softwood composition influences early-instar larval dispersal mortality during a spruce budworm outbreak. For. Ecol. Manage. **463**: 118035. doi:10.1016/j.foreco.2020.118035.